Transition metal defects in group-III nitrides: An *ab initio* calculation of hyperfine interactions and optical transitions

U. Gerstmann, A. T. Blumenau, and H. Overhof*
Theoretical Physics, Physics Department, University of Paderborn, D33095 Paderborn, Germany
(Received 18 August 2000; published 31 January 2001)

We present *ab initio* calculations for $3d$ transition metal point defects and for defect pairs in group-III nitrides with a special emphasis on charge transfer energies, hyperfine interactions, and internal optical transition energies. Our LMTO-ASA Green's function total energy calculations show Vac_N-TM pairs to be tightly bound in semiconducting and in n-type GaN and AlN with pair formation energies in excess of 1 eV. We show that in the framework of density functional theory reliable total energies are obtained for excited states, if the levels involved are represented by a single determinantal state within a $3d^N$ basis. Our optical transition energies agree fairly well with the experiments.

DOI: 10.1103/PhysRevB.63.075204 PACS number(s): 71.55.Eq, 76.30.Fc

I. INTRODUCTION

The large direct bandgap, ranging from 1.9 eV for InN to 6.2 eV for AlN makes the group-III nitride semiconductors attractive for many optoelectronic applications.[1,2] In spite of a considerable scientific effort, the characterization of the point defects in this material system is still quite incomplete. Several experimental groups have studied the optical and magneto-optical properties of the omnipresent $3d$ transition metal (TM) defects. However, even the chemical origin of several experimentally well studied zero phonon lines (ZPLs) is still a matter of controversy.[3] Since a detailed theoretical investigation of $3d$ TM defects is still missing, we present in this paper the results of a theoretical total energy calculation for both ground states and excited states of TM-related defects based on the local spin density approximation (LSDA) of the density functional theory (DFT).

The DFT can be used to calculate total energies of the ground state and for those excited states that are orthogonal by reasons of symmetry to the lower-lying states. This has been demonstrated recently for the $^5A_2$ excited state of the neutral vacancy in diamond.[4] Total energies and hyperfine (hf) fields of the excited state are obtained with a similar precision as the hf interactions for the ground state.

In this paper we investigate whether the same method can be extended to excitation energies of intra $3d$-shell transitions of TMs in order to support the identification of the chemical nature of the TM defects that give rise to ZPL lines. In Sec. II we sketch the general method used to calculate total energies for the multiplets of $3d$ TM defects. The resulting charge transfer levels, hyperfine interactions, and transition energies into excited states of $3d$ TM-related defects are presented in Sec. III and summarized in Sec. IV.

II. COMPUTATIONAL

We have used the self-consistent linear muffin-tin orbitals method in the atomic spheres approximation (LMTO-ASA)[5] treating exchange and correlation effects within the framework of the LSDA-DFT. To this aim Dyson's equation for the Green's function G for the crystal with a defect

$$G(\vec{r},\vec{r}\,',E)=G^0(\vec{r},\vec{r}\,',E)+\int G^0(\vec{r},\vec{r}\,'',E)\Delta V(\vec{r}\,'')G(\vec{r}\,'',\vec{r}\,',E)d^3r'' \tag{1}$$

is written in terms of the Green4s function G^0 of the perfect crystal. Here $\Delta V=V-V^0$ is the defect-induced change in the effective one-particle potentials. Equation (1) is solved within a perturbed region containing 28 atoms centered around the impurity. Outside this region, G is approximated by G^0.

A solution of Eq. (1) using the LMTO-ASA representation leads to accurate particle and magnetization densities, especially in the regions near the nuclei. From these we calculate hf interactions for paramagnetic defect states with the magnetic moments of the defect and ligand nuclei.[6,7] A main shortcoming of the LSDA, the underestimation of the fundamental band gap, is coped by the use of the scissors operator technique[8,9] when constructing the Green's function of the unperturbed crystal:

$$G^0_{\rm sc}(\vec{r},\vec{r}\,',E)=\int\frac{\psi^*(\vec{r},E')\psi(\vec{r}\,',E')}{E-\mathbf{O}_{\rm sc}E'}dE', \tag{2}$$

where $\mathbf{O}_{\rm sc}$ is the scissors operator adjusting the energy of the fundamental gap to the experimental value, but leaving the eigenfunctions unchanged. In this way the scissors operator technique simulates the GW-approximation,[10,11] a method that is widely used to improve the LSDA predictions of the fundamental gap and excited state energies.[12,13] We shall see that the use of the scissors operator leads to reasonable values for transition energies of defects in group-III nitrides.

Usually, isolated $3d$ TM defects are incorporated at the substitutional cation sites in group-III nitrides,[3] with four nitrogen atoms in tetrahedral configuration as nearest neighbors both for the zinc-blende and the wurtzite modifications. The strong localization of the $3d$ TM defect states leads to minor differences only for defects in different polytypes, as is confirmed by Ref. 14. In fact, most experimental papers discuss the $3d$ TM defect states in wurtzite group-III nitrides

 ©2001 The American Physical Society

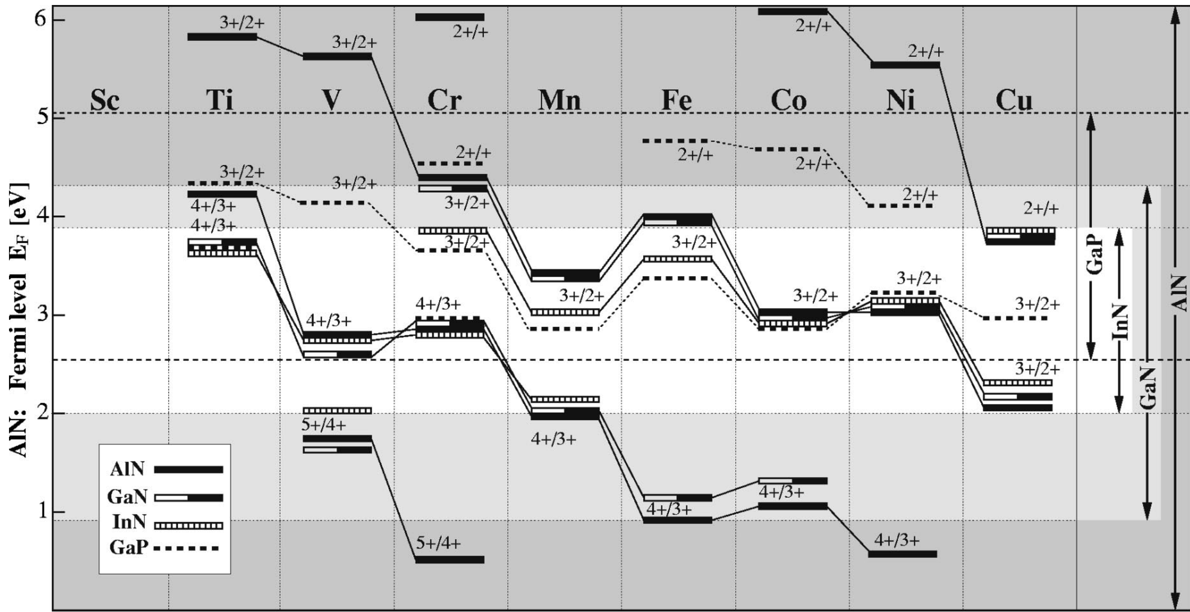

FIG. 1. Calculated charge transfer levels of isolated $3d$ TM defects in group-III nitrides. The valence and conduction band edges determined via the Langer-Heinrich rule using $Cr^{4+/3+}$ as reference level are indicated. For GaP experimental data taken from Refs. 22 and 27 are shown for comparison.

in terms of cubic symmetry. We, therefore, have restricted our calculations to defects in the zinc-blende structure. The semi-core character of the Ga $3d$- and In d-derived bands[15–17] presents no particular difficulty in our present approach, since we have treated the d-bands of the host as ordinary valence bands.

In its present form, our method does not allow to include lattice relaxations. For the gallium vacancy in GaN as an example we have calculated the lattice relaxation with the help of a density-functional-based tight-binding cluster calculation.[18] We obtained a 12% outwards relaxation of the next neighbor nitrogens and a change of the total energy of $\Delta E^{\mathrm{tot}}_{\mathrm{relax}} = -0.76$ eV. Since this value is practically independent of the charge state, there is only a minute influence of lattice relaxations on charge transfer levels. For $3d$ TM defects in semiconductors Langer[19] has shown lattice relaxations to influence energy differences like charge transfer levels by less than 0.1 eV—a value which is within the limits of accuracy of LSDA energy levels.

TM defects in semiconductors induce deep localized $3d$-like impurity states. The cubic crystal field splits the corresponding single particle states into states that transform according to the e and to the t_2 irreducible representations, respectively. These are further split by the exchange interaction into spin-up and spin-down states.

While the charge state of the defect uniquely fixes the number N of occupied $3d$-orbitals, the occupation of the different single particle states requires some care. A diagonalization with respect to the Coulomb interaction within the $\{e^n t_2^{N-n}\}$ subspace results in ${}^{(2S+1)}\Gamma(L)$ terms. This has been demonstrated by Tanabe and Sugano[20] who replace the matrix of Coulomb interactions by the free-atom Racah-parameters and treat the influence of the crystal field in first order perturbation theory.

In special cases a given ${}^{(2S+1)}\Gamma(L)$ term can be constructed by a single $e^n t_2^{N-n}$ determinantal many-particle wave function. In this case we approximate the energy of this term by the LSDA total energy of the corresponding $e^n t_2^{N-n}$ configuration. In the general case the ${}^{(2S+1)}\Gamma(L)$ term is to be constructed as a linear combination of several different $e^n t_2^{N-n}$ determinants in the d^N subspace. Configuration interactions will modify the energy of the ${}^{(2S+1)}\Gamma(L)$ term and the particle density distribution can no longer be approximated by a Kohn-Sham representation. With our present approach we have no means to calculate those term energies. Fortunately, most defect states of interest turn out to be single determinantal states within the d^N subspace.

III. RESULTS AND DISCUSSION

A. Isolated 3d TM defects in group-III nitrides

The internal reference rule of Langer and Heinrich[21,22] predicts the absolute positions of the charge transfer levels in different isovalent compound semiconductors to be independent of the host. One may shift the zero of the energy scale for different hosts in such a way, that the energies of a particular reference charge transition for a particular defect coincide. After this alignment of the energy scales, the energy of an arbitrary charge transition level for an arbitrary TM defect coincides for all hosts according to the Langer-Heinrich rule. Furthermore, this alignment provides us with an estimate for the valence and conduction band offsets.

Figure 1 summarizes the charge transfer energies calculated for isolated $3d$ TM defects incorporated at the substitutional cation sites in AlN, GaN, and InN. As is customary in ionic compounds like the group-III nitrides, the $3d$ TM defect state is characterized by its oxidation state rather than

TABLE I. Calculated and experimental valence band offsets (in eV) for group-III nitrides in the zinc-blende (ZB) and wurtzite (WZ) structures.

	AlN/GaN	GaN/InN	AlN/InN
LMTO[a] (ZB)	0.85	0.51	1.09
LAPW[b] (ZB)	0.84	0.26	1.04
LAPW[b](WZ)	0.81	0.48	1.25
Exp.[c] (WZ)	1.36±0.07		
Exp.[c] (WZ)		1.26±0.23	
Exp.[d] (WZ)	0.70±0.24	1.05±0.25	1.81±0.20
This work (ZB)	0.91	1.05	2.05

[a]Albanesi *et al.* (1994), Ref. 23.
[b]Wei and Zunger (1996), Ref. 24.
[c]Waltrop and Grant (1996), Ref. 25.
[d]Martin *et al.* (1996), Ref. 26.

by the charge state (however, when discussing pairs of $3d$ TM defects and vacancies, we shall label the vacancy by its charge state although its TM partner is labeled by its oxidation state). In Fig. 1 the $Cr^{4+/3+}$ donor level was taken as a reference level for the alignment of the band edges of all host materials. Figure 1 shows that the rule is a good approximation, especially for the acceptor levels $Co^{3+/2+}$ and $Ni^{3+/2+}$, and also for the the donor level $V^{4+/3+}$. From the Langer-Heinrich rule we estimate the valence band discontinuities for cubic AlN/GaN, GaN/InN, and AlN/InN materials to be 0.91, 1.05, and 2.05 eV, respectively.

In Table I a comparison of experimental valence band offsets with theoretical calculations of the interfaces by supercell calculations is given. All entries in Table I are positive, i.e., a larger band gap corresponds to a lower position of the valence band edge. Our estimate using the Langer-Heinrich rule for the AlN/GaN heterojunction leads to a band offset that is comparable to results of state-of-the-art calculations.[23,24] For the combinations with InN, our estimated offsets differ by a factor of two from the other theoretical results, but are in fair agreement with the band offsets determined by x-ray photoemission spectroscopy (XPS).[26]

Also included in Fig. 1 are the experimentally determined charge transfer levels of TMs in GaP which were taken from.[22,27] We have included these entries in order to show the internal reference rule to be less reliable if one combines group-III nitrides with other III-V semiconductors [see, e.g., the $(3+/2+)$ first acceptor levels of Ti, V, and Cu and especially the $(2+/+)$ second acceptor levels]. The reason may be the difference in electronegativity between nitrogen (3.04) and phosphorus (2.19).[28]

Experimentally, little is known about the charge transfer energies of $3d$ TM defects in group-III nitrides. The $Fe_{Ga}^{3+/2+}$ acceptor level in GaN e.g. has been determined by Baur *et al.*[29,30] to be at $E_v+2.5$ eV from the PL excitation spectra. This result has been challenged by Heitz *et al.*[31] who place the $Fe_{Ga}^{3+/2+}$ level 3.17 eV above the valence band. Our result of $E_v+3.14$ eV is in better agreement with Heitz *et al.*

The spin state of the $3d$ TM defect ground states is not as complex in the nitrides as it was in silicon:[9,32] for the d^N states with $N=3,4,5,6$ both high-spin and low-spin configurations are possible depending on the relative value of the exchange and crystal field splittings for the one-particle states. We find for almost all isolated $3d$ TM defects a high-spin ground state, similar to the model of Ludwig and Woodbury[33] for $3d$ TM defects in Si. There is one exception: the ground state of Fe^{4+} turns out to be diamagnetic with an energy difference of 0.4 eV to the $S=4/2$ high-spin state.

TABLE II. Hyperfine interactions (in MHz) for substitutional Mn_{Ga}^{2+} in GaN calculated with different LSDA and GGA parametrizations (see text).

	^{55}Mn(0,0,0)	^{14}N(1,1,1)		^{69}Ga(2,2,0)		
	a	a	b	a	b	b'
LSDA(CA)	−98.9	1.4	0.24	43.0	2.00	0.02
LSDA(PW)	−105.1	1.1	0.22	42.5	1.99	0.03
GGA(PBE96)	−85.6	0.6	0.21	41.5	1.87	0.13
mod. GGA	−228.5	0.4	0.21	39.8	1.85	0.13
Exp. Ref. 35	209.9					

B. hf interactions

Only a few deep defects in GaN have been observed by EPR: the $3d$ TM defects Ni, Fe, and Mn[28,34,35] have been identified, however, the hyperfine structure was resolved for the Mn impurity only.

The EPR spectrum with resolved hf structure[35,36] shows an $S=5/2$ high-spin state interacting with the central nuclear spin $I=5/2$ at 100% natural abundance. This proves that the defect is Mn_{Ga}^{2+}. The isotropic hf interaction with the ^{55}Mn nucleus calculated for Mn_{Ga}^{2+} is by a factor of two smaller than the experimental value of 210 MHz. A similar discrepancy is generally observed for $3d$ TM point defects in silicon and II-VI semiconductor compounds.[37,38] For $3d$ TM defects the isotropic hf interaction is caused by the spin polarization of the core states and the LSDA assumption of a homogeneous spin density is of course most strongly violated in the core regions. Thus, gradient corrections to the LSDA are expected to influence the magnetization density in the core region predominantly.[39–41] In Table II we have collected our hf interaction results obtained by using the LSDA parametrizations of Ceperley and Alder [LSDA(CA)][42] and the parametrization of Perdew and Wang [LSDA(PW)].[43] Also included are results using the GGA functional of Perdew, Burke, and Ernzerhoff [GGA(PBE96)].[44]

The incorporation of the GGA did not lead to a significant improvement of our results with respect to the LSDA values, probably because only the radial part of the gradient was taken into account in our calculation. We have simulated nonradial contributions by enhancing the radial gradient by about 20% in the region where the magnetization density is nonspherical. This procedure increases the modulus of the isotropic hf interaction with the ^{55}Mn defect nucleus to a value that is slightly larger than the experimental value, while leaving the hf interactions with the ligand nuclei al-

TABLE III. Hyperfine interactions with the ^{27}Al nucleus (in MHz) for selected intrinsic radiation defects ($S=1/2$) in AlN compared with experimental data. In the case of Vac_N^{2+} the interaction with the ^{27}Al ligand nucleus is shown. Theoretical results shown have been obtained using the LSDA and the modified GGA, respectively.

	^{27}Al (LSDA)		^{27}Al (mod. GGA)	
	a	b	a	b
Exp. Mason Ref. 51	66.7	19.7		
Exp. Honda Ref. 49	32.7			
Vac_N^{2+}	33.4	10.7	34.4	9.9
Al_{int}^0	11.3	8.6	11.9	7.9
$Vac_N^{2+}Al_{int}^0$	338.6	23.2	340.1	22.7

most unaffected. The success of this empirical correction strongly suggests a correct consideration of the nonradial contributions.

We note that the GGA correction affects only the hf interactions for d-like TM defects[45] for which the isotropic hf interaction is caused by the core polarization. The hf interactions for defects with isotropic hf interactions arising from s-like defect states are practically unaffected by GGA corrections (see also Table III).

As in most III-V compound semiconductors, the high abundance of paramagnetic host nuclei in GaN leads to broad EPR lines. Hence the hf splitting for many $3d$ TM defects like Fe cannot be resolved. Our calculated hf interaction of 13.5 MHz for the experimentally observed $Fe_{Ga}^{3+}(S=5/2)$ state predicts the hf splitting to be within the linewidth of the central EPR line,[35,36] even if we allow a factor-of-two correction. Thus, we suspect that doping with isotopically enriched ^{57}Fe will not resolve the hf splitting.

For AlN the number of deep defects with resolved hf interaction is slightly higher than for GaN. Baur *et al.*[46] observed an isotropic EPR signal in polycrystalline AlN ceramics[47] with $g=1.997$ and with a clearly resolved hyperfine structure. Besides the central line, there are at least four lines with a 53.51 MHz hyperfine splitting. The relative intensities are consistent with ^{53}Cr exclusively ($I=3/2$ and 9.5% natural abundance). We have shown recently for ^{53}Cr, that five different d^N states ranging from $N=1$ to $N=5$ can, in principle, account for these splittings.[37]

In ceramic AlN samples,[48] Honda *et al.*[49,50] have investigated the Vac_N^{2+} (F-center) radiation defect. A hf interaction with the ^{27}Al ligand of 32.7 MHz deduced from a linewidth analysis is in excellent agreement with our calculated value of 33.4 MHz (see Table III). Furthermore, for Vac_N^{2+} the optical excitation energy between the $^2A_1$ ground state and the $^2T_2$ excited state, calculated to be 3.69 eV, is in close agreement with the experimental value of 3.35 eV.[49]

A series of at least twelve EPR signals labeled D1 to D12 was reported by Mason *et al.*[51] Unfortunately, only for the D5 center with $S=1/2$ an anisotropic hf interaction ($A_\perp=47$ MHz and $A_\parallel=106$ MHz) could be resolved. From the shape of the EPR signal Mason *et al.* assigned the spectrum to a defect involving a magnetic nucleus of 100% abundance

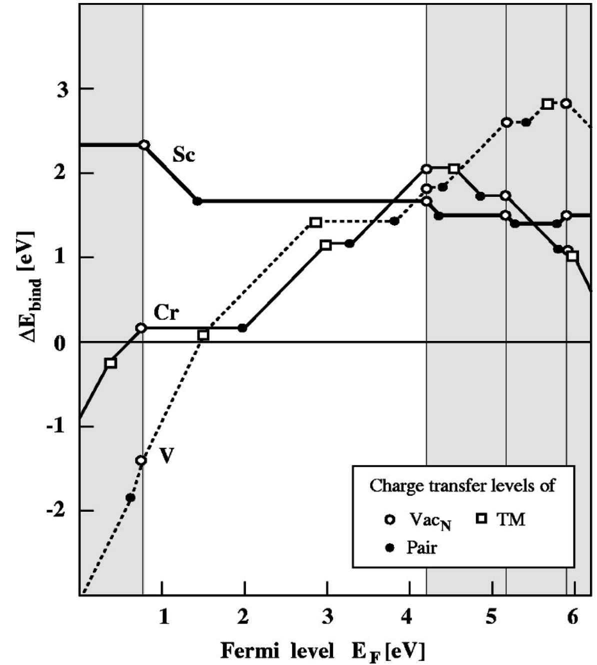

FIG. 2. Pair formation energies of various trigonal $Vac_N TM$ complexes in AlN, as a function of the Fermi energy. Full circles mark the charge transfer levels for the pairs, while empty circles and empty boxes mark the corresponding values for the isolated Vac_N and TM defects, respectively.

with I in the $3/2<I<7/2$ range. In some samples the D5 signal appeared after electron irradiation, suggesting the presence of an intrinsic radiation defect, as, e.g., the Al self-interstitial ($I=5/2$).

From our results we can exclude interstitial Al: for isolated Al_{int}^0 the calculated hf interaction values are too small while for the trigonal $Vac_N^+Al_{int}^0$ pair the respective values are much larger than the experimental data (see Table III).

The fact that D5 signals are observed exclusively in samples of low purity suggests extrinsic impurities to be involved, most likely trapped by radiation defects. Since our total energy calculations show $3d$ TM atoms and nitrogen vacancies to form stable impurity pairs in group-III nitrides, we have investigated vacancies paired with $3d$ TM partners that have 100% abundance for the isotope with a nuclear spin of about $I=5/2$: ^{45}Sc, ^{51}V, and ^{59}Co with nuclear spin 7/2, and ^{55}Mn with nuclear spin 5/2. We find five possible pair states with $S=1/2$: $Vac_N^+Mn_{Al}^{4+}$, $Vac_N^+Co_{Al}^{4+}$, $Vac_N^+V_{Al}^{2+}$ in a low-spin configuration and in addition $Vac_N^{2+}Sc_{Al}^{3+}$ and $Vac_N^+V_{Al}^{4+}$ in high-spin configurations. Figure 2 displays the pair formation energy of some pairs as a function of the Fermi energy.

For the pairs we use the convention that for the vacancy the charge state is given while for the $3d$ TM the oxidation state is given. This notation is not unique, $Vac_N^+Mn_{Al}^{4+}$ could equally well be denoted by $Vac_N^{2+}Mn_{Al}^{3+}$, but since the paramagnetic state of the pair closely resembles that of isolated Mn_{Al}^{4+}, we prefer the former notation (for the $Vac_N^{2+}Sc_{Al}^{3+}$ pair the Sc_{Al}^{4+} oxidation state would be quite unlikely, we shall see below that the magnetic state of this pair mimics that of the isolated Vac^{2+}).

TABLE IV. Hyperfine interactions (in MHz) for trigonal $3d$ TM impurity-vacancy pairs in AlN with $S=1/2$ compared with the experimental hf interaction for the D5 defect.

		TM(LSDA)		TM(mod. GGA)	
	I	a	b	a	b
Exp. Mason Ref. 51		66.7	19.7		
$\mathrm{Vac}_{\mathrm{N}}^{2+}\mathrm{Sc}_{\mathrm{Al}}^{3+}$	7/2	71.1	20.0	66.1	20.5
$\mathrm{Vac}_{\mathrm{N}}^{+}\mathrm{Mn}_{\mathrm{Al}}^{4+}$	5/2	−14.9	7.3	−32.8	8.2
$\mathrm{Vac}_{\mathrm{N}}^{+}\mathrm{V}_{\mathrm{Al}}^{2+}$	7/2	−96.3	30.9	−217.9	36.1
$\mathrm{Vac}_{\mathrm{N}}^{+}\mathrm{V}_{\mathrm{Al}}^{4+}$	7/2	−41.3	−76.3	−155.2	−73.3
$\mathrm{Vac}_{\mathrm{N}}^{+}\mathrm{Co}_{\mathrm{Al}}^{4+}$	7/2	−121.2	−104.7	−208.2	−94.4

A comparison of experimental and theoretical values for the hf interactions of these pairs in Table IV shows the $\mathrm{Vac}_{\mathrm{N}}^{2+}\mathrm{Sc}_{\mathrm{Al}}^{3+}$ pair to be a likely candidate for D5: isolated $\mathrm{Sc}_{\mathrm{Al}}^{3+}$ has a single spinless $3d^0$ electronic configuration with the first $3d$ single particle state high up in the conduction band. It therefore constitutes an extremely localized perturbation of the otherwise perfect crystal and is not easily observed experimentally. If $\mathrm{Sc}_{\mathrm{Al}}^{3+}$ is substituted for one nearest Al neighbor of $\mathrm{Vac}_{\mathrm{N}}^{2+}$, the resulting $\mathrm{Vac}_{\mathrm{N}}^{2+}\mathrm{Sc}_{\mathrm{Al}}^{3+}$ pair still is predominantly a vacancy-like defect, in contrast to the other $\mathrm{Vac}_{\mathrm{N}}^{+}$TM pairs. This is illustrated by the induced particle densities (see Fig. 3). Furthermore, the EPR-active oxidation state of the pair (which exists in thermal equilibrium for p-type samples with a Fermi level below 1.35 eV) is predicted to be very stable with a pair formation energy of about 2.3 eV. Thus, in this rather indirect way, electron radiation might activate the visibility of a Sc contamination in group-III nitrides.

C. Zero Phonon Lines in GaN and AlN

The experimental identification of $3d$ TM defects in group-III nitrides has progressed mainly by detailed investigations of the magneto-optical properties. The close analogy of several PL characteristics in GaN and AlN, especially the fact that the ZPLs appear at about the same energy in both materials, suggests a common assignment in both materials.

1. Vanadium related defects

For the ZPL at 0.94 eV, PLE and magneto-optical measurements[46,52,53] clearly prove a d^2 configuration with a $^3A_2$(F) ground state. According to our results only $\mathrm{Cr}_{\mathrm{Ga}}^{4+}$ and $\mathrm{V}_{\mathrm{Ga}}^{3+}$ offer a $3d^2$-configuration among the isolated $\mathrm{TM}_{\mathrm{Ga}}$ defects in GaN (see also Fig. 1). From our results we cannot exclude $\mathrm{Cr}_{\mathrm{Ga}}^{4+}$. However, the similarity of the 0.94 eV emission in GaN with the PL spectra of V^{3+} in other III-V compounds (GaAs, GaP, and InP) suggests this line to be due to $\mathrm{V}_{\mathrm{Ga}}^{3+}$.[52]

For a $3d^2$ system, seven different configurations can be combined into twelve many-particle terms. Fortunately, besides the ground state $^3A_2(F)$, also the exited states $^3T_2(F)$ and $^3T_1(P)$ can be expressed as a single determinantal configuration[20] (see also Fig. 4). The ground state $^3A_2(F)$ is constructed from the $e_{\uparrow}^2$ configuration. According to our calculations the $^3T_2(F)$ excited state (which is the ground state in the subspace $e_{\uparrow}^1 t_{2\uparrow}^1$) gives rise to a level which is about 1.12 eV above the ground state, a value that compares well with the experimental value of 0.931 eV given by Baur *et al.*[52] (see Table V).

The same authors reported additional absorption bands at 2.54 and 2.75 eV.[46] Diagonalizing empirical crystal-field matrices they tentatively assigned these transitions to absorptions into $^1T_2(D)$ and $^3T_1(P)$ excited states of isolated $\mathrm{V}_{\mathrm{Ga}}^{3+}$. In fact, for the $^3T_1(P)$ excited state which is the single determinantal ground state within the subspace of $t_{2\uparrow}^2$ configurations, our LSDA prediction is 2.67 eV, in close agreement with the experimental value.

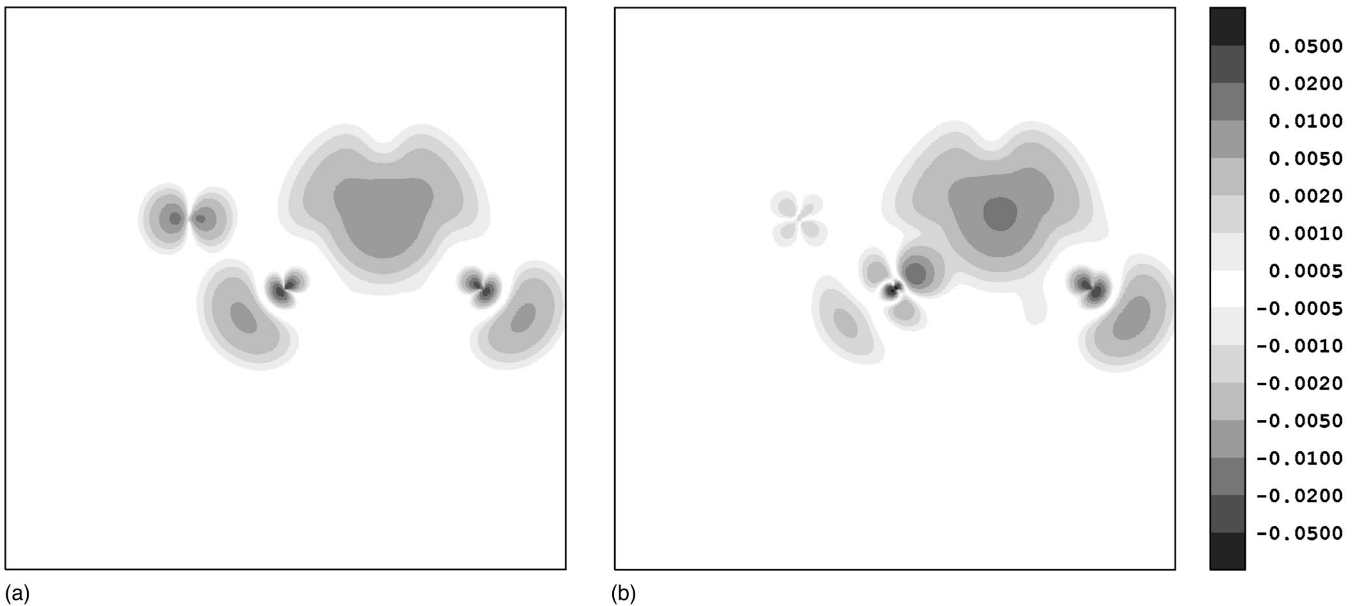

FIG. 3. Contour plots of the induced particle densities in the (110) plane. Part (a) shows the magnetization density of the isolated $\mathrm{Vac}_{\mathrm{N}}^{2+}$ and (b) the magnetization density of the $\mathrm{Vac}_{\mathrm{N}}^{2+}\mathrm{Sc}_{\mathrm{Al}}^{0}$ complex.

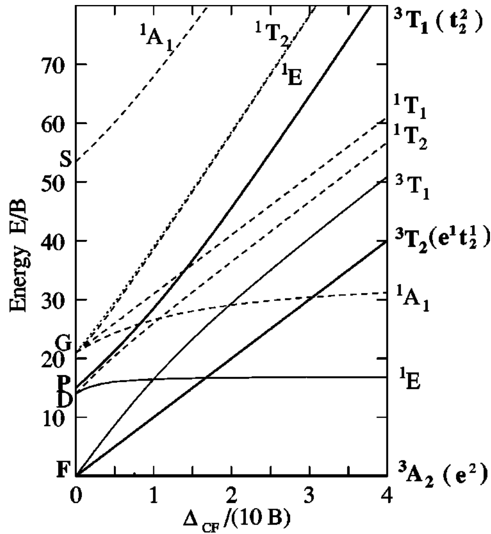

FIG. 4. Energy levels for $3d^2$ configurations (Tanabe-Sugano diagram) from Ref. 20.

While in temperature-dependent studies for GaN a hot line was detected at 1.6 meV above the main peak at 0.931 eV, for AlN no such hot line has been found. Hence, for AlN the corresponding excited state was attributed to a spin-singlet $^1E(F)$.[53] According to the Tanabe-Sugano diagram for $3d^2$ systems (see Fig. 4), a slightly higher crystal-field splitting of AlN as compared to GaN accounts for this change of symmetry for the first excited state. Unfortunately the determination of the energy of the $^1E(D)$ state, which cannot be represented by a single determinantal, is beyond the scope of this work.

Whereas in most semiconductors a variety of $3d$ TM defects can be introduced by various techniques, these techniques are less successful in the III-nitrides.[54–56] Only Vanadium implantation studies by Kaufmann *et al.*[57] have lead to a new, obviously V_{Ga}-related ZPL at 0.820 eV. An analogous ZPL in AlN was found at 0.797 eV.[53] This strongest PL in the series of TM related peaks is observed in semiconducting samples exclusively. A similar series of PL lines in ZnSe was assigned to the different oxidation states of isolated V_{Zn} point defects.[58,59]

According to our calculations, isolated V_{Ga} in GaN can have three different $3d^N$ states with $N=0$, 1, and 2. The V_{Ga}^{3+} oxidation state was already used for the explanation of the ZPL at 0.931 eV, while for the $3d^0$ configuration there is no state to be excited. For the remaining V_{Ga}^{4+} oxidation state there is a single transition $(^2T_2-^2E)$, which according to our calculations has a transition energy of 1.33 eV, clearly higher than the corresponding value in the V_{Ga}^{3+} oxidation state. Alternatively, we propose that the 0.82 eV ZPL is due to vanadium paired with a nitrogen vacancy, created as a radiation defect.[53,57] According to our calculations, Vac_N^+-TM complexes are stable in group-III nitrides with formation energies of about 1 eV in n-type and semiconducting samples (see also Fig. 2).

TABLE V. Excitation energies (in eV) of vanadium-related defects in GaN and AlN.

			LSDA	Exp.
V_{Ga}^{3+}	$^3T_2(F)$	$e_{\uparrow}^1 t_{2\uparrow}^1 e_{\downarrow}^0 t_{2\downarrow}^0$	1.12	0.931
	$^1T_2(D)$			2.54
	$^3T_1(P)$	$e_{\uparrow}^0 t_{2\uparrow}^2 e_{\downarrow}^0 t_{2\downarrow}^0$	2.67	2.75
$Vac_N^+ V_{Ga}^{3+}$	$^3A_1(F)$	$a_1^2 e_{\uparrow}^1 t_{2\uparrow}^1 e_{\downarrow}^0 t_{2\downarrow}^0$	0.80	0.820
V_{Al}^{3+}	$^1E(D)$			0.943
$Vac_N^+ V_{Al}^{3+}$	$^3A_1(F)$	$a_1^2 e_{\uparrow}^1 t_{2\uparrow}^1 e_{\downarrow}^0 t_{2\downarrow}^0$	0.72	0.797

In analogy to the interpretation of the 0.931 eV emission, the luminescence is expected to occur between a trigonally distorted $^3T_2(F)$ excited state and the distorted $^3A_2(F)$ ground state. For this transition, our LSDA estimates are 0.80 and 0.72 eV for the ZPL in GaN and AlN, respectively, in fair agreement with the experiments. In thermal equilibrium this charge state of the TM-vacancy pair exists for semiconducting samples with a Fermi level in the range between 0.99 and 2.71 eV above the valence band edge.

For a tightly bound trigonal pair the admixture between the vacancy-related and TM-related states is surprisingly small. This is illustrated in Fig. 5, where the induced particle density is split into contributions from states that transform according to the a_1 and e irreducible representations of C_{3v}. Whereas the density derived from a_1 states resembles that of an isolated Vac_N (see also Fig. 3), the density of the e states is typical for d-like orbitals.

2. Iron related ZPLs in GaN and AlN

ESR, ODMR, Zeeman, and photoluminescence (PL) investigations have shown[28,29] the 1.299 eV ZPL in GaN to be due to a $[^4T_1(G)-^6A_1(S)]$ transition of the $3d^5$ electron system of isolated Fe_{Ga}^{3+}. The high-spin ground state is confirmed by our self-consistent calculations. There can be no excited states with $S=5/2$, and therefore optical transitions into this state are spin-forbidden.

In a study of optical excitations for isolated Fe_{Ga} defects in GaN, Heitz *et al.*[31] found two intra-$3d$ transitions at 2.009 and 2.731 eV. These can be assigned to a $^4T_2(G)$ and a $^4E(G)$ excited state, respectively, according to the level ordering of the Tanabe-Sugano diagram for a $3d^5$ configuration.[20]

Describing the $^4T_1(G)$ excited state by an $e_{\uparrow}^2 t_{2\uparrow}^2 e_{\downarrow}^1$ configuration, we obtain a transition energy of 0.97 eV for the transition from $^4T_1(G)$, the excited state with lowest energy, into the $^6A_1(S)$. For the analogous Fe_{Al}^{3+} in AlN we obtain a transition energy of 1.12 eV in reasonable agreement with the experimental value of 1.297 eV. The energy of the $^4T_2(G)$ state if approximated by that of the $e_{\uparrow}^2 t_{2\uparrow}^2 t_{2\downarrow}^1$ configuration gives a transition energy of 2.04 eV, very close to the experimental value of 2.009 eV. Again, the $^4E(G)$ exited state cannot be treated within our simple approach.

In Table VI our results are compiled using both the LSDA and the modified GGA functionals for exchange and correlation. The modified GGA predicts transitions energies which are by about 0.1 eV higher than the corresponding LSDA values. Whereas our modified version of the GGA

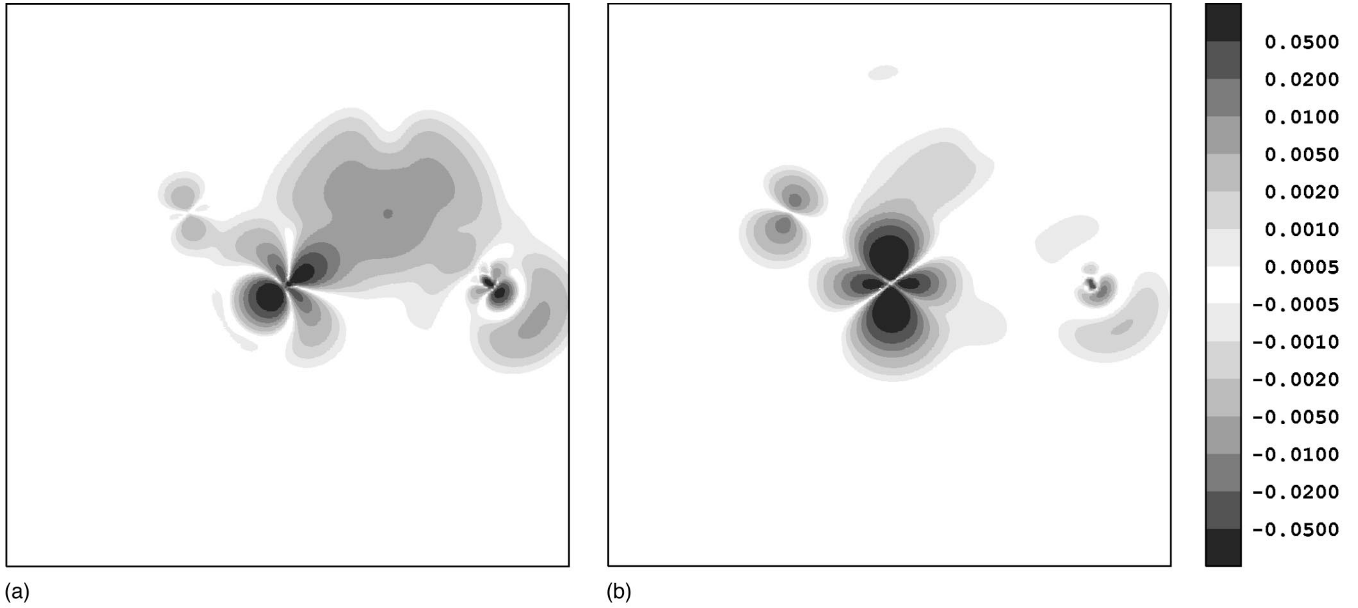

FIG. 5. Contour plots of the induced particle densities of the $Vac_N^+ V_{Ga}^{3+}$ in GaN in a (110) plane. Shown is the density due to states that transform according to the a_1 irreducible representation of C_{3v} in (a), and to the e representation in (b).

leads to a factor-of-two enhancement of the central isotropic hf interaction parameters, the same correction hardly affects the calculated transition energies.

3. The ZPL at 1.2 eV in GaN and AlN

The 1.2 eV ZPL can be identified as an intracenter $[{}^1E(D)-{}^3A_2(F)]$ transition within a $3d^2$-configuration of an isolated TM.[60] The assignment to Cr^{4+} as in Refs. 46 and 61 or to Ti^{2+} impurities, proposed by Refs. 31 and 62 on the other hand, is still controversial.

Baur *et al.*[46,52] assign this ZPL in AlN to isolated Cr_{Al}^{4+} because of the correlation between this emission and the Cr-related EPR signal in AlN: after neutron irradiation, causing a change of the Fermi level because of radiation defects, the Cr-related EPR signal disappears while simultaneously the 1.201 eV ZPL increases dramatically.

The observed broadening of additional lines near 1.2 eV in Cr-doped GaN samples was explained by the presence of Cr-related defect pairs.[46,52] This suggestion is corroborated by our finding of stable pairs of Cr with Vac_N: we predict four different charge states, a fact that could explain the occurrence of several additional lines. For the single positive charge state of the pair we obtain transition energies of 1.16 and 1.13 eV in GaN and AlN, respectively. Here we assume a $[{}^3A_1(F)-{}^3A_2(F)]$ transition of the $3d^2$ configuration in analogy with the excitation mechanism for the $Vac_N^+V^{3+}$ complex.

Heitz *et al.*[60] observed an effective excitation of the 1.193 eV emission via higher excited states at 1.7 and 2.8 eV in *n*-type GaN samples. Their proposal that Ti_{Ga}^{2+} is responsible for the 1.193 eV transition must be questioned on the basis of our results: We do not find the Ti_{Ga}^{2+} oxidation state in GaN. In *n*-type GaN, only V_{Ga}^{3+} has a $3d^2$ configuration, a defect state that was already shown to be responsible for the 0.931 eV emission.

Therefore, an assignment to Cr_{Ga}^{4+} appears to be the most probable possibility. The excitation energies for Cr_{Ga}^{4+} are summarized in Table VII. The high excitation efficiency for the 1.193 eV emission in *n*-type samples requires the presence of other defects coupled to Cr_{Ga}^{4+} by generation or capture of holes. Two-color stimulation experiments e.g. prove energy transfer between the yellow luminescence (YL) and Fe_{Ga}^{3+} centers by hole transfer.[63]

TABLE VI. Excitation energies (in eV) of iron-related defects in GaN and AlN. The theoretical results are obtained using the LSDA and the modified GGA approximations.

			LSDA	mod. GGA	Exp.
Fe_{Ga}^{3+}	${}^4T_1(G)$	$e_\uparrow^2 t_{2\uparrow}^2 e_\downarrow^1 t_{2\downarrow}^0$	0.97	1.04	1.299
	${}^4T_2(G)$	$e_\uparrow^2 t_{2\uparrow}^2 e_\downarrow^0 t_{2\downarrow}^1$	2.04	2.05	2.009
	${}^4E(G)$				2.731
Fe_{Al}^{3+}	${}^4T_1(G)$	$e_\uparrow^2 t_{2\uparrow}^2 e_\downarrow^1 t_{2\downarrow}^0$	1.12	1.30	1.297

TABLE VII. Excitation energies (in eV) for chromium-related defects in GaN and AlN.

			LSDA	Exp.
Cr_{Ga}^{4+}	${}^1E(D)$			1.193
	${}^3T_1(F)$			1.6
	${}^3T_1(P)$	$e_\uparrow^0 t_{2\uparrow}^2 e_\downarrow^0 t_{2\downarrow}^0$	2.69	2.8
$Vac_N^+Cr_{Ga}^{4+}$	${}^3A_1(F)$	$a_1^2 e_\uparrow^1 t_{2\uparrow}^1 e_\downarrow^0 t_{2\downarrow}^0$	1.16	1.188
Cr_{Al}^{4+}	${}^1E(D)$			1.201

Based upon this observation Heitz *et al.*[31] claim the capture of holes h_{vb} to be the excitation process of the Fe^{3+}_{Ga} luminescence in n-type samples:

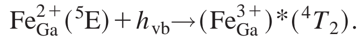

$$Fe^{2+}_{Ga}(^5E)+h_{vb}\rightarrow(Fe^{3+}_{Ga})^*(^4T_2).$$

A similar mechanism for Cr^{3+}_{Ga} in n-type GaN would end up in the $^3A_2$ ground state of the 1.193 eV emission:

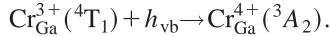

$$Cr^{3+}_{Ga}(^4T_1)+h_{vb}\rightarrow Cr^{4+}_{Ga}(^3A_2).$$

Starting from this $^3A_2(F)$ ground state various excitation processes are possible, especially an efficient recharging process into the neutral charge state Cr^{3+}_{Ga} for which we calculate a charge transfer energy of about 1.98 eV and last but not least the observed excitation of the 1.193 eV luminescence via the spin- and symmetry-allowed transitions into the $^3T_1(F)$ (1.7 eV excitation) and $^3T_1(P)$ (2.8 eV excitation) terms. Therefore, the absorption between 1.6 and 2.0 eV might be attributed to a superposition of the bands due to the absorption $[^3A_2(F)-{}^3T_1(F)]$ and a recharging process into the neutral charge state.

Unfortunately, the $^3T_1(F)$ excited state cannot be described as a ground state of a symmetry subspace, preventing an estimate for the $[^3A_2(F)-{}^3T_1(F)]$ excitation energy. However, the next higher lying $^3T_1(P)$ excited state is the ground state within the subspace of the $t^2_{2\uparrow}$ configuration. Our calculation places this absorption into the blue/green spectral range—namely 2.69 eV, in fair agreement with the experimental value of about 2.8 eV.

4. The ZPL at 1.045 eV in GaN and AlN

The 1.045 eV ZPL shows the clear fingerprint of a $[^4T_2(F)-{}^4A_2(F)]$ transition due to a $3d^7$ configuration of an isolated TM in GaN.[56] According to our total energy calculations, only Co^{2+}_{Ga} and Ni^{3+}_{Ga} offer a $^4T_2(F)$ ground state of the d^7 electronic configuration. The n-type samples used by Pressel *et al.*,[56] grown using a modified sublimation sandwich technique,[64] contain Fe, Cr, Ti, and Ni as unintentional defects. The 1.047 eV ZPL was observed after excitation at 1.6 eV without a detectable charge transfer process and was tentatively assigned to Co^{2+}_{Ga}.[56] In fact, according to our calculations, in n-type GaN at thermal equilibrium only Co^{2+}_{Ga} can be in a $3d^7$ state, but Co is not considered to be a dominant contamination in these samples. Also, the presence of Ni^{3+}_{Ga} after the capture of holes generated by other centers cannot be excluded.

The excited $^4T_2(F)$ term in both cases can be well approximated as the ground state of the $e^2_{\uparrow}t^3_{2\uparrow}e^1_{\downarrow}t^1_{2\downarrow}$ subspace. For Ni^{2+}_{Ga} we obtain a transition energy of 1.14 and 1.04 eV for GaN and AlN, respectively, in fair agreement with the experimental values of 1.043 and 1.047 eV. The calculated estimates for Co^{2+}_{Ga} are only about 0.2 eV too low in energy. Therefore, the previous assignment[34,36] of the emissions near 1.045 eV to isolated Ni^{3+}_{Ga} centers is not really unique.

IV. CONCLUSIONS

We have shown that for $3d$ TM defects in group-III nitrides most of the optical ZPL can be interpreted consistently on the basis of *ab initio* calculations using the general LSDA framework. At least for those excited states that can be regarded as single-determinantal ground state of some d^N configuration, the LSDA total energies provide a reasonable approximation of the state energies. We further have shown that an accurate estimate of the various band offsets can be made combining our defect charge transfer level positions with the assumption that the Langer-Heinrich rule is strictly valid within the group-III nitrides. Comparison with data for GaP shows that the ionic group-III nitrides are distinctly different from the conventional III-V compound semiconductors.

ACKNOWLEDGMENT

One of the authors (U.G.) is grateful for financial support by a grant of the Deutsche Forschungsgemeinschaft (DFG).

*Electronic mail: h.overhof@phys.upb.de

[1] When speaking about group-III nitrides, we exclude BN which has physical properties that differ from AlN, GaN, and InN.

[2] S. J. Pearton, J. C. Zolper, R. J. Shul, and F. Ren, J. Appl. Phys. **86**, 1 (1999).
[3] B. K. Meyer, A. Hoffmann, and P. Thurian, in *Group III Nitride Semiconductor Compounds*, edited by B. Gil, *Series on Semiconductors Science and Technology*, Oxford (1998).
[4] U. Gerstmann, M. Amkreutz, and H. Overhof, Phys. Rev. B **60**, R8446 (1999).
[5] O. Gunnarsson, O. Jepsen, and O. K. Andersen, Phys. Rev. B **27**, 7144 (1983).
[6] H. Weihrich and H. Overhof, Phys. Rev. B **54**, 4680 (1996).
[7] M. Illgner and H. Overhof, Phys. Rev. B **54**, 2505 (1996).
[8] G. A. Baraff and M. Schlüter, Phys. Rev. B **30**, 3460 (1984).
[9] F. Beeler, O. K. Andersen, and M. Scheffler, Phys. Rev. B **41**, 1603 (1990).
[10] L. Hedin, Phys. Rev. **139**, A796 (1965).
[11] L. Hedin and S. Lundqvist, in *Solid State Physics*, edited by F. Seitz, D. Turnbull, and H. Ehrenreich (Academic Press, New York, 1969), Vol. 23, p. 1.
[12] M. S. Hybertsen and S. G. Louie, Phys. Rev. B **34**, 5390 (1986).
[13] R. W. Godby, M. Schlüter, and L. J. Sham, Phys. Rev. B **37**, 10 159 (1988).
[14] T. Mattila and R. M. Nieminen, Phys. Rev. B **55**, 9571 (1997).
[15] V. Fiorentini, M. Methfessel, and M. Scheffler, Phys. Rev. B **47**, 13 353 (1993).
[16] A. F. Wright and J. S. Nelson, Phys. Rev. B **50**, 2159 (1994).
[17] W. R. L. Lambrecht, B. Segall, S. Strite, G. Martin, A. Agarwal, H. Morkoc, and A. Rockett, Phys. Rev. B **50**, 14 155 (1993).
[18] M. Elstner, D. Porezag, G. Jungnickel, J. Elsner, M. Haugk, Th. Frauenheim, S. Suhai, and G. Seifert, Phys. Rev. B **58**, 7260 (1998).
[19] J. M. Langer, in *New Developments in Semiconductor Physics*, edited by F. Beleznay, G. Ferenczi, and J. Giber, *Lecture Notes in Physics* (Springer, New York, 1988), Vol. 122, p. 123.

[20] S. Sugano, Y. Tanabe, and H. Kamimura, *Multiplets of Transition-Metal Ions in Crystals* (Academic Press, New York, 1970).
[21] J. M. Langer and H. Heinrich, Phys. Rev. Lett. **55**, 1414 (1985).
[22] J. M. Langer, C. Delerue, M. Lannoo, and H. Heinrich, Phys. Rev. B **38**, 7723 (1988).
[23] E. A. Albanesi, W. R. L. Lamprecht, and B. Segall, MRS Soc. Proc. **339**, 604 (1994).
[24] S. H. Wei and A. Zunger, Appl. Phys. Lett. **69**, 2719 (1996).
[25] J. R. Waldrop and R. W. Grant, Appl. Phys. Lett. **68**, 2879 (1996).
[26] G. Martin, A. Botchkarev, A. Rockett, and H. Morkoc, Appl. Phys. Lett. **68**, 2541 (1996).
[27] B. Clerjaud, in *Semiconductor Physics*, edited by A. M. Stoneham, *Current Issues in Solid State Sciences* (A. Hilger, Bristol and Boston, 1986), p. 117.
[28] R. Heitz, P. Thurian, I. Loa, L. Eckey, A. Hoffmann, I. Broser, K. Pressel, B. K. Meyer, and E. N. Mokhov, Appl. Phys. Lett. **67**, 2822 (1995).
[29] K. Maier, M. Kunzer, U. Kaufmann, J. Schneider, B. Monemar, I. Akasaki, and H. Amano, Mat. Sci. Forum **143-147**, 93 (1994).
[30] J. Baur, K. Maier, M. Kunzer, U. Kaufmann, and J. Schneider, Appl. Phys. Lett. **65**, 2211 (1994).
[31] R. Heitz, P. Maxim, L. Eckey, P. Thurian, A. Hoffmann, I. Broser, K. Pressel, and B. K. Meyer, Phys. Rev. B **55**, 4328 (1997).
[32] F. Beeler, Ph.D. thesis, Universität Stuttgart (1986).
[33] G. W. Ludwig and H. H. Woodbury, Solid State Phys. **13**, 223 (1962).
[34] P. G. Baranov, I. V. Ilyin, and E. N. Mokhov, Solid State Commun. **101**, 611 (1997).
[35] P. G. Baranov, I. V. Ilyin, E. N. Mokhov, and A. D. Roenkov, Semicond. Sci. Technol. **11**, 1843 (1996).
[36] P. G. Baranov, I. V. Ilyin, and E. N. Mokhov, Mater. Sci. Forum **258-263**, 1167 (1997).
[37] U. Gerstmann, M. Amkreutz, and H. Overhof, Phys. Status Solidi B **217**, 665 (2000).
[38] M. Illgner and H. Overhof, Semicond. Sci. Technol. **11**, 977 (1996).
[39] S. Blügel, H. Akai, R. Zeller, and P. H. Dederichs, Phys. Rev. B **35**, 3271 (1987).
[40] H. Ebert, P. Strange, and B. L. Gyorffy, Z. Phys. B: Condens. Matter **73**, 77 (1988).
[41] M. Battocletti, H. Ebert, and H. Akai, Phys. Rev. B **53**, 9776 (1996).
[42] D. M. Ceperley and B. J. Alder, Phys. Rev. Lett. **45**, 566 (1980).
[43] J. P. Perdew and Y. Wang, Phys. Rev. B **33**, 8800 (1986); **40**, 3399 (1989); **45**, 13 244 (1992).
[44] J. P. Perdew, K. Burke, and M. Ernzerhof, Phys. Rev. Lett. **77**, 3865 (1996).
[45] U. Gerstmann and H. Overhof, Physica B **273-274**, 88 (1999).
[46] J. Baur, U. Kaufmann, M. Kunzer, J. Schneider, H. Amano, I. Akasaki, T. Detchprohm, and K. Hiramatsu, Mater. Sci. Forum **196-201**, 55 (1995).
[47] M. Kuramoto and H. Taniguchi, J. Mater. Sci. Lett. **3**, 471 (1984).
[48] M. Kuramoto, H. Taniguchi, and I. Aso, Ceram. Bull. **68**, 883 (1989).
[49] M. Honda, K. Atobe, N. Fukuoka, M. Okada, and M. Nakagawa, Jpn. J. Appl. Phys., Part 2 **29**, L652 (1990).
[50] K. Atobe, M. Honda, N. Fukuoka, M. Okada, and M. Nakagawa, Jpn. J. Appl. Phys., Part 1 **29**, 150 (1990).
[51] P. M. Mason, H. Przybylinska, and G. D. Watkins, Phys. Rev. B **59**, 1937 (1999).
[52] J. Baur, U. Kaufmann, M. Kunzer, J. Schneider, H. Amano, I. Akasaki, T. Detchprohm, and K. Hiramatsu, Appl. Phys. Lett. **67**, 1140 (1995).
[53] P. Thurian, I. Loa, P. Maxim, K. Pressel, A. Hoffmann, I. Broser, and C. Thomsen, Mat. Sci. Forum **258−263**, 1131 (1997).
[54] J. I. Pankove and J. A. Huchby, J. Appl. Phys. **47**, 5387 (1976).
[55] B. Monemar and O. Lagerstedt, J. Appl. Phys. **50**, 6480 (1979).
[56] K. Pressel, S. Nilsson, R. Heitz, A. Hoffmann, and B. K. Meyer, J. Appl. Phys. **79**, 3214 (1996).
[57] B. Kaufmann, A. Dörnen, V. Härle, H. Bolay, F. Scholz, and G. Pensl, Appl. Phys. Lett. **68**, 203 (1996).
[58] G. Goetz, U. W. Pohl, and H. J. Schulz, J. Phys. C **4**, 8253 (1992).
[59] G. Goetz, U. W. Pohl, H. J. Schulz, and M. Thiede, J. Lumin. C **60−61**, 16 (1994).
[60] R. Heitz, P. Thurian, K. Pressel, I. Loa, L. Eckey, A. Hoffmann, I. Broser, B. K. Meyer, and E. N. Mokhov, Phys. Rev. B **52**, 16 508 (1995).
[61] J. Baur, K. Maier, M. Kunzer, U. Kaufmann, J. Schneider, H. Amano, I. Akasaki, T. Detchprohm, and K. Hiramatsu, Appl. Phys. Lett. **64**, 857 (1994).
[62] K. Pressel, R. Heitz, L. Eckey, I. Loa, P. Thurian, A. Hoffmann, B. K. Meyer, S. Fischer, C. Wetzel, and E. E. Haller, MRS Symp. Proc. **395**, 491 (1995).
[63] A. Hoffmann, L. Eckey, P. Maxim, J.-Chr. Holst, R. Heitz, D. M. Hofmann, D. Kovalev, G. Stevde, D. Volm, B. K. Meyer, T. Detchprohm, K. Hiramatsu, H. Amano, and I. Akasaki, Solid-State Electron. **41**, 275 (1997).
[64] Y. A. Vodakov, E. N. Mokhov, A. D. Roenkov, and D. T. Saidbekov, Phys. Status Solidi A **51**, 209 (1979).